

# Platform for High-Throughput Testing of the Effect of Soluble Compounds on 3D Cell Cultures

Frédérique Deiss,<sup>†,‡</sup> Aaron Mazzeo,<sup>†</sup> Estrella Hong,<sup>†</sup> Donald E. Ingber,<sup>§,||</sup> Ratmir Derda,<sup>\*,†,‡,§</sup> and George M. Whitesides<sup>\*,†,§</sup>

<sup>†</sup>Department of Chemistry and Chemical Biology, Harvard University, Cambridge, Massachusetts 02138, United States

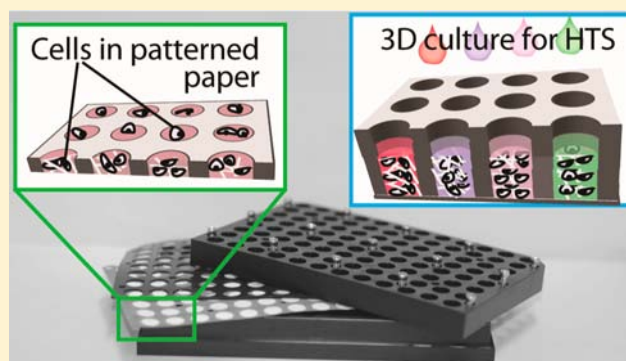
<sup>‡</sup>Department of Chemistry, University of Alberta, Edmonton, AB T6G 2G2, Canada

<sup>§</sup>Wyss Institute for Biologically Inspired Engineering at Harvard University, Harvard Medical School, and Boston Children's Hospital, Boston, Massachusetts 02115, United States

<sup>||</sup>Harvard School of Engineering and Applied Sciences, Cambridge, Massachusetts 02139, United States

## S Supporting Information

**ABSTRACT:** *In vitro* 3D culture could provide an important model of tissues *in vivo*, but assessing the effects of chemical compounds on cells in specific regions of 3D culture requires physical isolation of cells and thus currently relies mostly on delicate and low-throughput methods. This paper describes a technique (“cells-in-gels-in-paper”, CiGiP) that permits rapid assembly of arrays of 3D cell cultures and convenient isolation of cells from specific regions of these cultures. The 3D cultures were generated by stacking sheets of 200- $\mu\text{m}$ -thick paper, each sheet supporting 96 individual “spots” (thin circular slabs) of hydrogels containing cells, separated by hydrophobic material (wax, PDMS) impermeable to aqueous solutions, and hydrophilic and most hydrophobic solutes. A custom-made 96-well holder isolated the cell-containing zones from each other. Each well contained media to which a different compound could be added. After culture and disassembly of the holder, peeling the layers apart “sectioned” the individual 3D cultures into 200- $\mu\text{m}$ -thick sections which were easy to analyze using 2D imaging (e.g., with a commercial gel scanner). This 96-well holder brings new utilities to high-throughput, cell-based screening, by combining the simplicity of CiGiP with the convenience of a microtiter plate. This work demonstrated the potential of this type of assays by examining the cytotoxic effects of phenylarsine oxide (PAO) and cyclophosphamide (CPA) on human breast cancer cells positioned at different separations from culture media in 3D cultures.



Cell-based assays that use cell cultures on 2D substrates are widely employed for drug development, tissue bioengineering, and fundamental studies of cellular functions. Cells cultured in 2D are, however, not an accurate model of the *in vivo* environment: cells cultured in a monolayer, on the flat rigid surface of a Petri dish, can have essential processes and cellular functions that are different from those in cells *in vivo*. The majority of cells in living organism grow in organized arrays, as three-dimensional structures (“tissues”), and surrounded by extracellular matrix (ECM). In the past 2 decades, 3D cell culture in ECM hydrogels has been developed extensively as an *in vitro* model with which to understand the behavior of cells *in vivo*.<sup>1</sup> Cells cultured in 3D in extracellular matrix (ECM) gels generate many of the original growth characteristics of the tissues and enable their evaluation under *in vivo*-like conditions.<sup>1–5</sup> As one example, Weaver et al. demonstrated that, in cancerous breast cells grown in 3D hydrogels, blocking the  $\beta 1$ -integrin receptor led to normalization of cell morphology and caused cells to organize into the polarized lumens formed by a noncancerous epithelial cell.<sup>6</sup> These

structures were never observed in 2D-culture.<sup>3,4,6</sup> Many other cell types, including tumor cells, chondrocytes, and embryonic stem cells require a 3D microenvironment to acquire morphology and physiology that resemble that of the same types of cells *in vivo*.<sup>7–10</sup>

There have been several reports of high-throughput systems that allow testing the effect of chemical compounds on the properties and phenotypic behaviors of cells cultured in 3D hydrogels.<sup>7,11–15</sup> The groups of Clark and Dordick proposed a high-throughput 3D cellular microarray for use in drug discovery, toxicity screening, and study of differentiation in stem cells.<sup>12,15,16</sup> These platforms, however, required specific equipment for preparing the miniaturized 3D cell culture arrays on functionalized glass slides (e.g., a microarray spotter) and for analyzing (e.g., scaled-down immunofluorescence techniques) the response of cells in a microwell to specific stimuli; even

Received: January 16, 2013

Accepted: July 12, 2013

Published: July 12, 2013

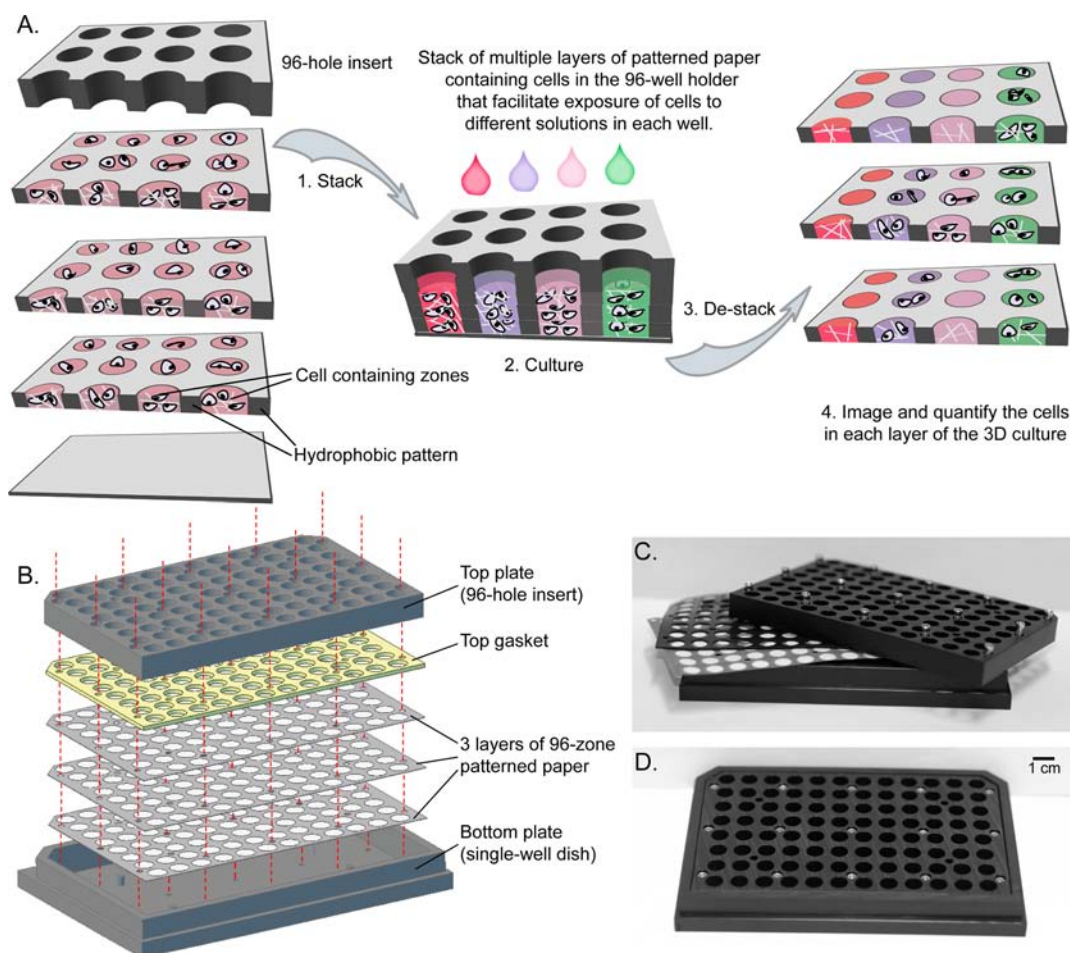


**Figure 1.** General design of the 96-well holder containing multiple sheets of paper impregnated with mammalian cells. Patterned papers with hydrophilic zones separated by hydrophobic barriers are stacked between a single-well dish and a 96-hole insert. The wells, capable of containing different media, are formed by the walls of the 96-hole insert. Hydrophobic barriers inside the paper prevent capillary wicking between the wells, and a soft hydrophobic gasket prevents wicking of liquids between the paper and the 96-hole insert. (A) Concept of the 96-well holder: In this scheme, the 3D cultures comprise a stack of three layers of paper, with each hydrophilic zone containing mammalian cells that are exposed to three replicates of four formulations of media. After culture, the three layers are destacked and the cells in each zone of the paper-based layers can be analyzed using a microscope, a fluorescent scanner, or a plate reader. (B) The scheme shows assembly of a single-well dish, a gasket, several patterned sheets of paper, and a 96-hole insert. After the individual components are stacked, bolts (represented by the red dashed lines) going through all the thickness of the assembly hold the stack together and provide the necessary compression to prevent leaking. (C and D) Photographs of a 96-well holder in Delrin before and after assembly.

with this complexity, they do not generate information on distinct responses of cells from different locations of the construct.<sup>16</sup> Microfluidic technology had been employed to allow monitoring of cells in microenvironments in real time and to study the spatial and temporal effects of chemical compounds.<sup>3,17–21</sup> These techniques are useful but not ideally convenient. High-throughput assays using the standard 96-well format are especially valuable, because they can be easily integrated with the well-established, commercially supported instrumental infrastructure for liquid-handling of cells and testing of compounds and for high-throughput analysis (e.g., scanners, plate readers, spectrophotometers, robots). These assays can use aggregated cells in gel particles distributed to individual wells or cells growing in thin gels on the surface of 96-well plates or 96-well inserts (e.g., Transwell assays); there are also several descriptions of microfluidic devices that are compatible with microplate readers.<sup>2,8,22–25</sup>

Most assays that combine 3D culture with a 96-well plate format provide rapid readout for the average response of cells from the wells that contain 3D constructs but do not provide

information either about cells in different regions of these 3D constructs or about other aspects of heterogeneous responses. Cells in distinct locations in 3D tissue, however, are physiologically and metabolically different, because they are exposed to different concentrations of oxygen, nutrients, signaling molecules, and mechanical stress.<sup>5,9</sup> These and other dissimilarities in local extracellular environments can result in major differences in behavior, and in responses of cells in different regions of 3D culture to bioactive chemical compounds such as drug candidates, environmental toxins, nutrients, and others. The behavior of cells in different locations of 3D constructs *in vitro* could mimic responses of cells *in vivo* in different locations of tissues (e.g., in poorly oxygenated tumors and in regions of infarct, inflammation, and other types of hypoxia).

Biochemical processing of cells, for example, immunostaining or metabolic staining in 3D culture, is significantly more complex than similar analysis of cells in 2D culture. These procedures could be performed only in constructs thinner than a few hundred micrometers because diffusion of reagents,

antibodies, or metabolic dyes through thick tissue constructs is slow.<sup>26,27</sup> In standard 3D culture, thus, characterizations of cells as a function of location in the 3D tissues require techniques such as microtomy or laser-capture microdissection to isolate thin, cell-containing slices or individual cells from different regions of 3D-cultures. These techniques, however, are inherently low-throughput and, in practice, usually allow only the processing of small numbers of samples.

To overcome these problems, we are developing a technique that we refer to as “cells-in-gels-in-paper” (CiGiP).<sup>28,29</sup> This technique can generate a continuous 3D “tissue” by stacking layers of paper impregnated with cell-containing hydrogels (e.g., Matrigel); the layers can be destacked to separate and simplify analysis of cells in specific regions of the 3D “tissue”.<sup>28</sup> A tissue generated using this approach could contain an organized array of one or multiple types of cells, supported by an analogue of extracellular matrix and mechanical fibers. The thickness of the slabs of gel supported by the matrix of cellulose fibers in one sheet of paper is similar to that of the paper (we typically use 200- $\mu\text{m}$ -thick paper). This thickness is relevant to the distances across which oxygen and nutrients diffuse within 3D tissues *in vivo*. In experimental demonstrations of CiGiP, growth of cells inside the 200- $\mu\text{m}$ -thick paper gel slabs was not limited by mass transport of oxygen and nutrients.<sup>28</sup> Stacking multiple layers assembled a thick tissue (thickness = number of layers  $\times$  thickness of one layer of paper) with vertical gradients of oxygen and nutrients, generated by metabolic activity of cells. Cells proliferated or died in response to local concentrations and migrated to follow these gradients.<sup>28,29</sup> CiGiP facilitated rapid isolation of live cells from 3D cultures as destacking the individual layers of paper (peeling the layers apart) “sectioned” these tissues and isolated the cells into 200- $\mu\text{m}$ -thick slabs.<sup>28,29</sup> We have further developed this convenient experimental technique by using sheets of paper patterned into 96 hydrophilic zones, surrounded by hydrophobic barriers.<sup>29</sup> It enabled parallel assembly and analysis of 96 3D cultures by stacking these 96-zone sheets and submerging them in a common medium in a Petri dish.<sup>29</sup> Exposure of individual cultures to different chemicals was not possible with this system.

In this article, we describe a holder for 96-zone, multilayer culture with a design similar to the “bottomless 96-well plate” manufactured, for example, by Greiner Bio-One. We assembled the holder by placing a grid containing 96 holes (96-hole insert) into a single-well dish that contained a stack of multiple layers of 96-zone patterned sheets of paper (Figure 1). Each well (hole) of the 96-hole insert was aligned with one of the hydrophilic regions of the 96-zone, patterned paper. Each well, thus, contained a continuous 3D tissue, consisting of multiple stacked slabs of cells in Matrigel, supported by the stack of layers of paper. The 96-well holder, assembled as described, allowed each tissue to be separated from the tissues in the neighboring wells. This arrangement makes it possible to expose each stacked 3D culture to a medium with a different formulation.

This separation is not complete because some molecules can diffuse laterally through pores in the hydrophobic wax, but it is adequate for many studies. We will describe alternative systems that lead to better isolation of zones, but with greater complexity in fabrication, in later papers. In this manuscript, we developed the 96-zone format to answer a main issue in the development of new techniques based on 3D cell cultures, which is their integration into the currently available laboratory

equipment.<sup>1,8</sup> The familiarity and convenience of a 96-well format will, we hope, accelerate the development of high-throughput assays for 3D cell cultures based on CiGiP (and other related techniques), first in research and later in clinical laboratories.

## ■ EXPERIMENTAL SECTION

**Design of the 96-Well Holders.** We had several requirements for the design of the holder containing 96 isolated multilayer cultures: (i) Fabrication of all components of the 96-well, multilayer holder must be simple and compatible with rapid, inexpensive techniques of fabrication (e.g., printing, injection molding). (ii) Individual multilayer cultures in a stack of multizone arrays of cells in gels must be isolated from one another. Stacking should minimize capillary wicking of fluids atop or inside the paper. (iii) To make automation of high-throughput analyses of cells in these cultures possible, plating of cells, and stacking and destacking of the cultures, must involve only manipulations sufficiently simple that they, in principle, could be executed by the robots commonly used in high-throughput screening.

We generated multiple prototypes of the holder in acrylonitrile butadiene styrene (ABS) using a 3D printer (Dimension Elite from Stratasys) and then ordered versions machined in other materials for the most successful designs. The bottom half of the holder has the footprint of a single-well dish (e.g., similar to the Nunc OmniTray), and can house several sheets of paper that contain arrays of cells in gels (Figure 1B). The top plate is a 96-hole insert, which, when placed on top of the stacked layers of paper and gasket(s), completes the assembly and yields a 96-well holder for stacks of 96-zone papers. The top and bottom halves of the 96-well holders were fastened together with 15 bolts; this number of bolts was the minimum that would give an even pressure and block leakage by wicking between sheets of paper. An automatic screwdriver, sensitive to torque, allowed us to control and achieve reproducibly the necessary pressure (0.25 N m). Eliminating even 1 of the 15 bolts always led to leakage in the areas surrounding the missing bolt, and tensioning them correctly remains an experimental nuisance that would have to be simplified or eliminated in a fully rational design. Comparing leakage data from a configuration with two gaskets to a configuration with one gasket showed no improvements with an additional gasket; therefore, for all the experiments presented in this report, we used the simpler configuration with one gasket.

**Preparation of the Holders and the 96-Zone Layers for 96 3D Cell Cultures.** We patterned multizone papers and plated cells according to an already described procedure.<sup>29</sup> Human breast-cancer cells (MDA-MB-231) were suspended in Matrigel ( $5 \times 10^6$  cells/mL). Spotting 4  $\mu\text{L}$  of this suspension onto one hydrophilic zone of the multizone layers and warming the Matrigel to 36 °C generated a slab of paper-supported Matrigel, 6 mm in diameter and 200  $\mu\text{m}$  in thickness, which contained  $\sim 20\,000$  cells (confocal micrographs of the cells in paper along the *z*-axis are available in the Supporting Information, Figure S4 and the movie). The sheets of paper were then put in a dish containing growth medium and allowed time to equilibrate (overnight). All the elements of the holder (top and bottom plates, gasket, and screws) were autoclaved. The layers of paper supporting the arrays of 96 gels were stacked into the bottom plate, which had four posts to guide the alignment of the layers. We added the gasket and the top

plate and fastened the bolts. We added 200  $\mu\text{L}$  of medium to each well and placed the 96-well holders on an orbital shaker in an incubator at 36  $^{\circ}\text{C}$ , 5%  $\text{CO}_2$ .

**Testing the Toxicity of the Materials for the 96-Well Holder.** To evaluate the influence of selected materials (gaskets and plates) on the growth of mammalian cells plated in thin gels supported by paper, we placed a paper impregnated with Matrigel containing  $\sim 80\,000$  cells in a well of a 12-well plate and added  $\sim 1\text{ cm}^2$  sheets of the material to be tested. At different days (up to 10 days), we assessed the number of metabolically active cells using the rate of the turnover of the metabolic dye Alamar Blue (AB). The fluorescence of AB was recorded with a plate reader (Spectramax Gemini XS).

**Performance of the 96-Well Holder with a Toxic, Water-Soluble Compound.** We stacked three wax-patterned 96-zone cell-containing layers and a PDMS gasket inside the 96-well holder to generate 600  $\mu\text{m}$ -thick cultures within each well. For comparison, we also stacked a cell-containing layer in between two cell-free layers impregnated only with Matrigel. This procedure generated, in each well, a 600- $\mu\text{m}$ -thick gel with cells in a 200- $\mu\text{m}$ -thick section in the middle of the slab of gel. After assembling the 96-well holders, we added to each well growth medium containing phenylarsine oxide (PAO) at six different concentrations between 0 and 50  $\mu\text{M}$ . We cultured the cells for 24 h, disassembled the 96-well holders, and peeled the layers apart. We stained the layers with calcein-AM and scanned them with a fluorescent gel scanner (Typhoon FLA 9000, GE) to visualize viable cells in each zone. An automatic image-processing procedure in Matlab quantified images of arrays obtained from the gel scanner.<sup>29</sup> This custom-made image analysis software processed the images of multizone arrays and calculated the intensity of fluorescence in each zone and each layer. This value is proportional to the amount of calcein-AM turned over by metabolically active cells.

**Evaluation of the 96-Well Holder under Stringent Conditions.** To assess whether small hydrophobic molecules could diffuse between the wells, we tested the device in the presence of the small hydrophobic toxin used previously, PAO, present at concentration exceeding the toxic dose by a factor of  $>500$ . For this experiment, we stacked two 96-zone, paper-based layers that contained MDA-MB-231 cells in Matrigel. This procedure generated an array of 96 tissues, each of them in a 400- $\mu\text{m}$ -thick slab of Matrigel supported by the matrix of cellulose fibers of the paper. We filled every other well in one-half of the plate with medium that contained some PAO at a concentration of 250  $\mu\text{M}$ . The remaining wells of the plate contained regular growth medium. After 1 day of culture, we added AB to each well and recorded the fluorescence after 4 h. As the 96-well holder has the same footprint as a standard 96-well plate, we were able to measure fluorescence intensity of AB directly by placing the 96-well holder into the plate reader (Spectramax Gemini XS). We then analyzed the different sections of the tissues by destacking the assembly and visualizing the live cells inside each layer with calcein-AM, using the procedure explained in the previous experiment.

**Long-Term Exposure of Cells-in-Gels-in-Paper to Cyclophosphamide (CPA).** We cultured MDA-MB-231 GFP cells in three different configurations: (i) 2D culture in 96-well plate, (ii) 3D culture in a 200  $\mu\text{m}$ -thick single layer of paper gripped by 96-well holder, and (iii) 3D culture in a 600  $\mu\text{m}$ -thick, three-layer stack gripped by 96-well holder. For the 2D experiment, we plated 10 000 cells per well (150  $\mu\text{L}$  volume), allowed the cells to attach for 24 h, and added a

solution of CPA (concentration ranging from 0 to 7600  $\mu\text{M}$ , six replicas). After 3 days, we added Alamar blue (AB) to each well (1:10, v/v in media) and recorded the fluorescent intensity of the supernatant after 3.5 h using a plate reader. In CPA-free wells, cells were actively dividing and the number of cells increased significantly over the course of 3 days; we confirmed this increase both by microscopy and by measuring the AB turnover on day 0 and day 3.

For the 3D experiments, we impregnated the hydrophilic zones of 96-zone wax-patterned paper layers with a suspension of MDA-MB-231-GFP cells in a cold (4  $^{\circ}\text{C}$ ) mixture of growth media and Matrigel (1:1, v/v). We placed the layers in an excess of warm media (20 mm dish, 40 mL of media) and maintained the layers in these conditions for 24 h before stacking. To create 3D-1L constructs, we sandwiched one 96-zone paper in between two PDMS gaskets and gripped them inside a 96-well holder. For 3D-3L constructs, we sandwiched three 96-zone papers in between two PDMS gaskets and gripped them inside a 96-well holder. We cultured the cells for 24 h inside the holder and then treated each well with CPA (200  $\mu\text{L}$  of media + CPA per well). We removed the media daily and supplied fresh medium containing an appropriate concentration of CPA. After 3 days, we disassembled the holder, peeled the layers apart, and stained them with calcein (4  $\mu\text{g}/\text{mL}$  calcein in prewarmed serum-free MEM medium, 20 min incubation with gentle shaking at 36  $^{\circ}\text{C}$ ). The layers were scanned using Typhoon FLA9000 fluorescent gel scanner (473 nm excitation, long-pass blue (LPB) filter, PMT = 300 V, 100  $\mu\text{m}$  resolution). Image analysis of cell containing zones was performed in MatLab; the script and processing steps were adapted from our previous publication without any modifications.<sup>29</sup> The integrated intensities from zones that describe replica of the experiments were further processed by a separate MatLab script to generate the boxplot, which described the median, the 25th, and 75th percentile of the population and statistically validated outliers. This script is available in the Supporting Information.

## RESULTS AND DISCUSSION

**Testing the Performance of 96-Well Holders that Contained Paper Sheets.** Fastening ordinary (nonpatterned) paper between two halves of the 96-well holder does not eliminate leakage of liquid between the wells because liquid can wick and solutes diffuse, from well to well, either in the spaces between the paper and the holder or inside the paper. To circumvent the first problem, we used gaskets. The second problem can be circumvented by patterning the paper with hydrophobic barriers. We tested two approaches: (i) Using a commercially available solid ink (wax) printer (Phaser 8560DN, Xerox), we printed a wax pattern that outlined 96 wax-free circular zones (Figure S2 in the Supporting Information). Heating the paper (120  $^{\circ}\text{C}$ , 2 min) caused the wax to permeate the thickness of the paper by spreading along the surface of the cellulose fibers.<sup>30</sup> Although wax-permeated paper largely blocked permeation of aqueous solution from zone to zone, it did not block spreading of organic solvents nor completely block migration of small hydrophobic molecules. (ii) As this 96-well holder is not intended solely for applications based on cell-culture assay, we also studied solution to create patterns that could resist spreading of organic solvents. To this end, we used a rubber stamp to deposit a pattern of polydimethylsiloxane (PDMS) inside the paper. Other methods

Table 1. Tested Materials for Gaskets<sup>a</sup>

material	specifications	Shore A hardness (durometer)	thickness (in.)	abbreviation Figure 2	leakage <sup>b</sup>	toxic
PDMS	home-cast	N/A	~0.05	PDMS	+++	no
commercial PDMS	medical grade	40	0.02	PDMS MG	+++	no
natural latex rubber	abrasion-resistant	40	0.03	Latex	++	yes
high-strength Buna-N rubber	oil-resistant	40	1/16	–	++	N/A
high-strength Buna-N rubber	oil-resistant	40	1/32	Rubber 40a	+++	yes
super-resilient foam	quick-recovery	N/A	1/32	Foam	+++	yes
ultra-strength Buna-N rubber	oil-resistant	50	1/32	Rubber 50a	+	yes
high-strength Neoprene rubber	FDA-compliant	50	1/32	Neoprene	N/A	yes
Buna-N/vinyl rubber	FDA-compliant	70	1/32	BNV	N/A	yes
Santoprene rubber	FDA-compliant	55	1/32	Santoprene	++	no
Buna-N rubber	FDA-compliant	60	1/16	BN	N/A	yes
silicone rubber	medical grade	40	1/16	Sil. MG	+++	no

<sup>a</sup>All materials were bought from McMaster-Carr (NJ), except the home-cast PDMS, prepared from the bi-component elastomer Sylgard 184 Silicone, purchased from Essex Brownell (Edison, NJ), and the medical grade silicone rubber purchased from Diversified Silicone Products (Santa Fe Springs, CA). <sup>b</sup>+++ , 0 well leaking; ++, 1–2 wells leaking; +, 3–5 wells leaking.

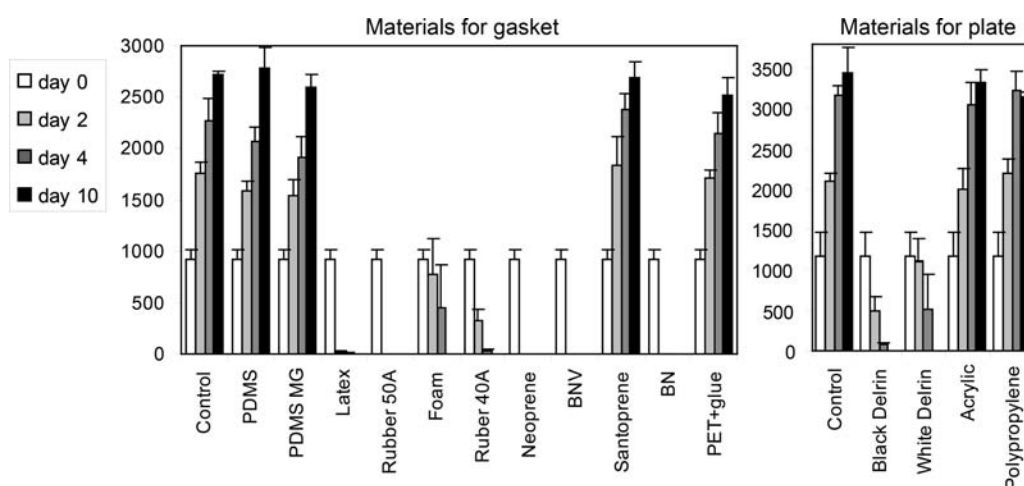


**Figure 2.** Toxicity of the materials of the 96-well holder. This toxicity study was realized on 10 potential materials for gaskets and 4 materials for plates (measured in separate experiments). The toxicity of the wax has been characterized in previous publications.<sup>29</sup> This wax has no measurable effect on cell growth. We placed a 1-cm<sup>2</sup> piece of material into a well containing paper impregnated with MDA-MB-231 cells in Matrigel (~80 000 cells on day 0). On the indicated days, we added metabolic dye (Alamar Blue) to the wells; after 5 h of incubation, we collected the reagent and measured its fluorescence (*y*-axis), which was proportional to the number of metabolically active cells in the dish. Data is the average from four replicates ( $N = 8$ , two collections of reagents per replica). Error bars are  $\pm 1$  standard deviation.

of patterning (e.g., plotting of PDMS,<sup>31</sup> SU-8 photolithography<sup>30</sup>) could possibly be used as well.

To evaluate these patterning techniques and different types of elastomers that might be used as gaskets, we monitored the leakage of aqueous solutions of dyes between the wells of the 96-well holder. Each holder consisted of a top (96-hole insert) and bottom (single well dish) sandwiching a sheet of patterned paper and gasket(s) (Table 1). The performance of PDMS-patterned papers was, on average, similar to that of wax-patterned paper. The patterning by wax, however, is simpler and faster in a lab-scale setting. We, thus, optimized all leakage tests using wax-patterned paper. The gaskets that prevented leakage best were made of moderately firm materials (Shore A hardness from 40 to 50). Evaluation of different stacked geometries (single or double gasket, single or multiple layers of paper) demonstrated that the pressure from a single, top, elastomeric gasket is sufficient to eliminate cross-contamination between the wells, i.e., we observed no leakage from one well to its neighbor along the paper. We envision that in an optimized design the gasket could be fused to the inner surface of the top

of the holder, to minimize the number of components necessary for assembly.

**Testing the Toxicity of the Materials for the 96-Well Holder.** We evaluated the influence of the materials (gaskets and plates) selected for assembly of the holder on the growth of mammalian cells over the course of 10 days (Figure 2). Most of the materials tested were claimed to be FDA-compliant by the manufacturer (i.e., made from ingredients or materials listed as approved by the Food and Drug Administration). Neoprene, Buna-N/vinyl, and Buna-N rubbers nonetheless induced cell death in less than 4 days. Materials for the gaskets that were nontoxic were Santoprene and siloxanes (PDMS and medical grade Silicone (not shown)).

Materials for the plates that seemed to be nontoxic were polypropylene and poly(methyl methacrylate) (PMMA) (Figure 2). All these materials had no effect on the growth of MDA-MB-231 cells over the duration of the assay. We selected PMMA plates because polypropylene deformed during autoclaving. The use of low-temperature sterilization techniques (e.g., radiation or ethylene oxide) would bypass this

limitation. For large-scale production, we envision a holder made of polystyrene that could be formed by injection molding.

We also examined whether the confinement induced by the 96-hole insert was affecting the CiGiP and determined it was not. Convective mixing of media in tall, narrow wells can be slower than that in shallow dishes; thus, the access of oxygen to cells in narrow wells might, in principle, be reduced. Figure S3 in the Supporting Information presents the comparison of 200- $\mu\text{m}$ -thick 3D cell cultures realized in different conditions of confinement and show that cells grew well when cultured in the 96-well holder.

**Performance of the 96-Well Holder for Testing Toxicity of Water-Soluble Compounds.** We tested the ability of the patterned-paper layers stacked in the assembled holders to prevent diffusion of cytotoxic small organic molecules between the wells during prolonged culture. In our previous reports, we characterized the morphology of MDA-MB-231 cells and other cell lines inside Matrigel slabs supported by paper<sup>28</sup> and quantified the distribution of these cells through individual 200- $\mu\text{m}$  thick sheets of Whatman 114 paper.<sup>29</sup> The paper acts only as an inert support with  $\sim 70\%$  void; hydrogel with trapped cells fill this void. In this article, we used Matrigel; however, other ECM gels, such as collagen or synthetic hydrogels, could also be used to impregnate paper. For the experiments presented in this manuscript, we used 96-well holders with three layers of paper containing cells and generated two arrays of 600- $\mu\text{m}$ -thick slabs, one with cells through the whole thickness (Figure 3B) and a second one containing cells only in the middle of the slabs, through 200  $\mu\text{m}$  (Figure 3D). We chose three layers constructs  $L_1L_2L_3$  of 600- $\mu\text{m}$ -thickness because this number of layers was shown to be sufficient to establish two phenotypically distinct populations of normoxic and hypoxic MDA-MB-231 cells.<sup>28</sup> In this present work, we further demonstrate that differences in the oxygenation level lead to different responses of the cells to the drugs.

As an example of a cytotoxic hydrophobic small molecule, we used phenylarsine oxide (PAO, structure in the Supporting Information). This molecule causes cell death in less than 12 h, at concentrations of  $\sim 5 \mu\text{M}$ , by inhibiting protein-tyrosine phosphatases and other bis-thiol-containing proteins.<sup>32,33</sup> Figure 3 displays images of the layers generated by the gel scanner after the exposition to PAO and analyses of the different sections of the cultures (In these images, the black color is proportional to green fluorescence). PAO at concentrations higher than 0.4  $\mu\text{M}$  killed breast cancer cells (MDA-MB-231) within 24 h. The relationship between the number of metabolically active cells and concentration of PAO follows a dose–response curve with apparent EC50 of  $\sim 1 \mu\text{M}$ . (Note: In this context, “EC50” stands for the half-maximal effective concentration, in mol/L, that induces a response halfway between the baseline and maximum). The behaviors of cells in different locations in the 3D cultures were different. Because of the gradient of distribution of oxygen in different layers,<sup>28,32</sup> the number of live cells in the top 200- $\mu\text{m}$ -thick layers (in direct contact with oxygenated medium) was 15% higher ( $p < 0.01$ ) than that in the layers more than 200  $\mu\text{m}$  away from the oxygenated medium (comparing “top”, “bot”, and “med” in Figure 3A,B; no PAO). The intermediate concentrations of PAO (0.4  $\mu\text{M}$ ) killed a significantly higher fraction of cells in the top layers (45%) than in the lower layers (20–25% for “mid” and “bot” layer, Figure 3A,B). In the presence of 0.4  $\mu\text{M}$  PAO, there was over 1.5-fold more cells ( $p < 0.01$ ) in the 200- $\mu\text{m}$ -thick sections surrounded by 200- $\mu\text{m}$ -

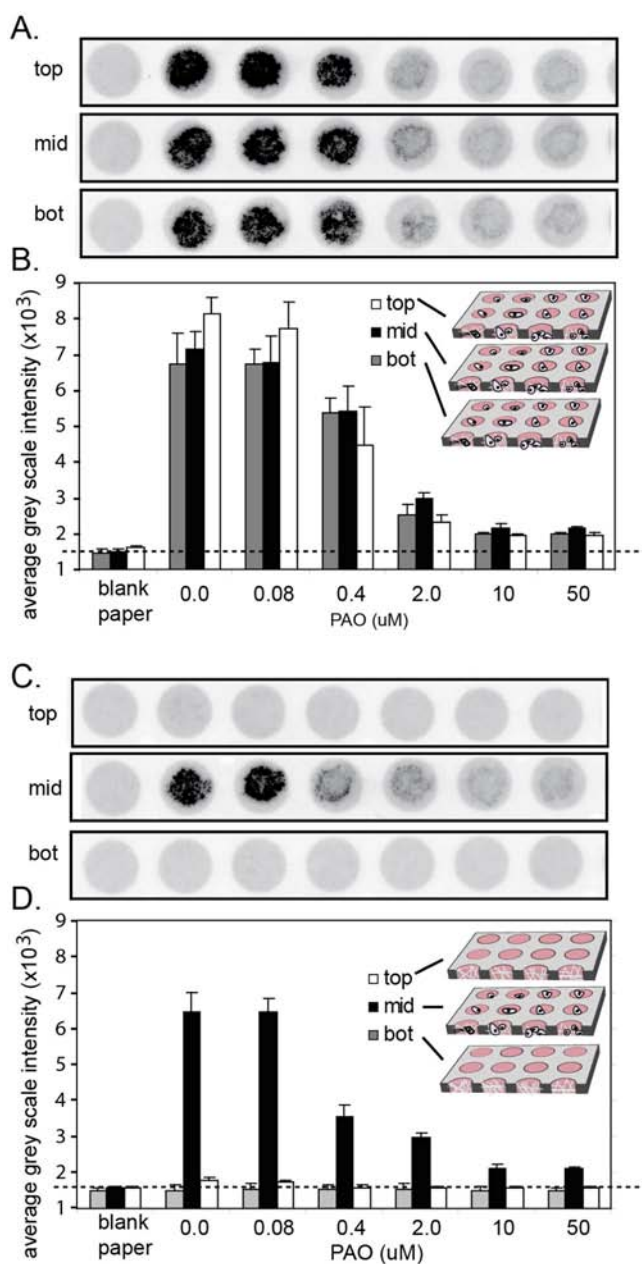


**Figure 3.** Fluorescence imaging and analysis after calcein-staining of 3D cultures exposed for a single day to different amount of phenylarsine oxide (PAO): (A,B) 3D culture of  $3 \times 200\text{-}\mu\text{m}$ -thick Matrigel slabs with MDA-MB-231 cells and (C,D) 200- $\mu\text{m}$ -thick Matrigel slabs with MDA-MB-231 cells between two 200- $\mu\text{m}$ -thick Matrigel slabs without cells. All constructs were treated with PAO for 24 h (different concentrations in different zones), destacked, stained with calcein, and imaged by a gel scanner. Parts A and C show representative images from the scanned layers (black color is proportional to green fluorescence). Parts B and D display the fluorescent intensity proportional to the number of metabolically active cells (the average gray scale intensity of each zone is then averaged across the 6 replica with the error bar presenting the standard deviation) at different concentrations of PAO. Most cells died at PAO concentrations  $> 10 \mu\text{M}$ . Cell death upon exposure to 0.4  $\mu\text{M}$  PAO depends on the relative location of cells in the 3D construct and its composition. Cells in the middle layer of a  $3 \times 200 \mu\text{m}$ -thick culture surrounded by cell-free Matrigel (C,D) were more susceptible to PAO than the same cells inside a  $3 \times 200\text{-}\mu\text{m}$ -thick culture surrounded by Matrigel and cells (A,B).

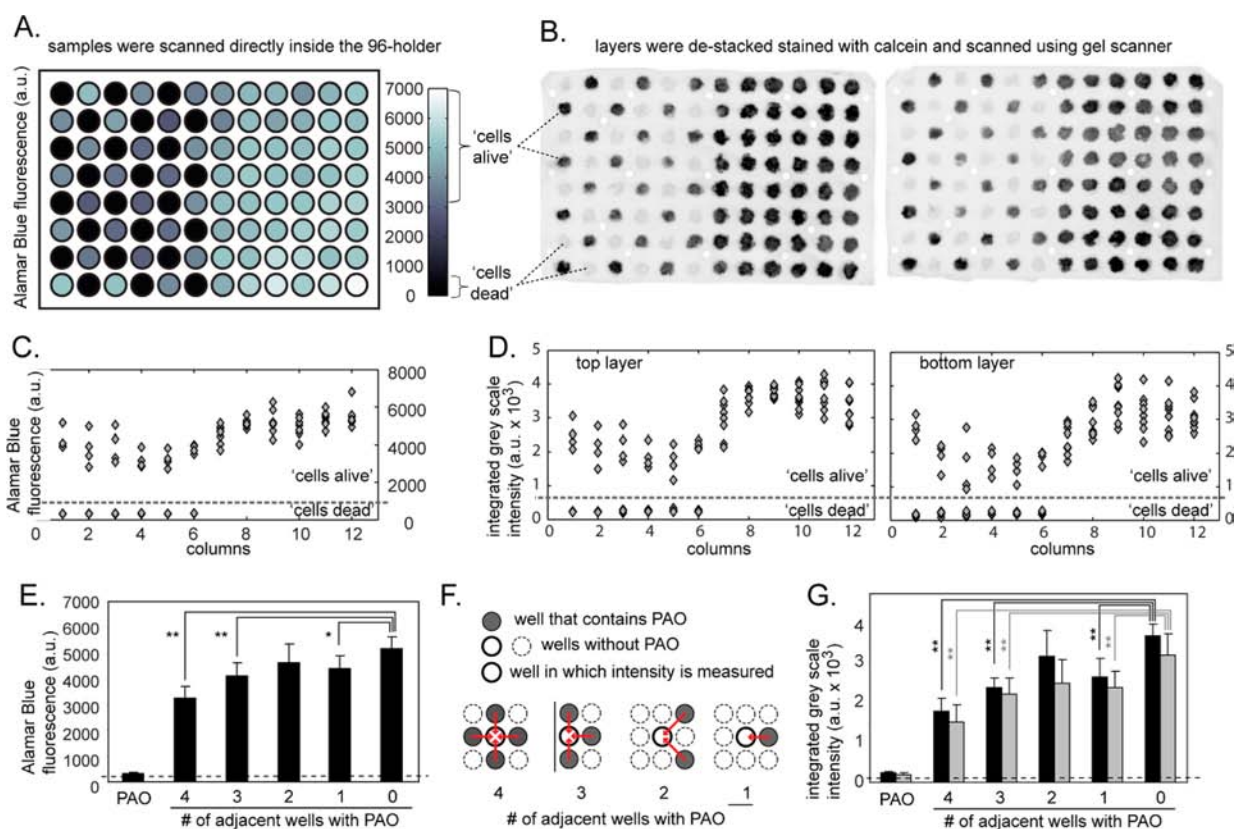


**Figure 4.** Binary test of cell cultures exposed to phenylarsine oxide (PAO). We stacked two 96-zone layers, which contained MDA-MB-231 GFP cells in each zone, inside the 96-well holder. To each well, we added either 200  $\mu\text{L}$  of medium containing 250  $\mu\text{M}$  of PAO or 200  $\mu\text{L}$  of toxin-free medium, following a half checkerboard pattern. After 1 day of incubation, we assessed the viability of the cells with Alamar blue (AB). The fluorescent intensity of AB was recorded after 4 h 15 min by placing the 96-well holder in a standard plate reader. Part A displays fluorescent intensities in the wells as a heat-map image with a reversed intensity scale. We then disassembled the 96-well holder, stained the two layers with calcein-AM, and imaged the fluorescent intensity of calcein in the layers using a gel scanner (B). Parts C and D plot numerical values of fluorescence from parts A or B. Parts E and G plot average intensity of Alamar Blue (E) or calcein signal (G) in wells that were adjacent to PAO-containing wells (black and gray bars correspond, respectively, to values from the top and bottom layer). Part F outlines examples of the layouts of wells that had 1, 2, 3, or 4 adjacent wells with PAO. The data in parts E and G is an average from 5 to 40 measurements. Error bars are  $\pm 1$  standard deviation. \*  $p < 0.05$ , \*\*  $p < 0.01$  as determined by two-tailed, nonequal variance, student  $t$ -test.

thick sections filled by cells (Figure 3A,B) than in the 200- $\mu\text{m}$ -thick sections which were surrounded by blank Matrigel slabs (Figure 3C,D). This observation confirmed that PAO, like other molecules consumed by cells, formed gradients in 3D cultures by kinetic processes that combine diffusion and “reaction” (for PAO, binding to proteins in cells) and not as a result of its slow diffusion through gels or paper.

**Performance of the 96-Well Holder under Stringent Conditions: Lateral Differences Between Zones.** Although the holder can resist spreading of dyes and blocks permeation of low concentrations of organic molecules between wells, we tested the device with an array of 96, 400- $\mu\text{m}$ -thick tissues under more stringent conditions (>500-fold excess of cytotoxic small molecules). We exposed the cultures to growth medium and to medium that was 250- $\mu\text{M}$  in PAO (a 250-fold higher concentration than the EC50) following a half checkerboard pattern (Figure 4).

After 1 day of culture, the analysis of each culture with AB showed that the wells treated with PAO contained no live cells, as they exhibited no fluorescence (Figure 4A). We destacked the assembly to analyze individually the two 200- $\mu\text{m}$ -thick sections of the cultures and confirmed the results of the AB/plate reader test: the half checkerboard pattern was clearly visible in the fluorescence gel-scanned images (Figure 4B).

Furthermore, measuring the intensities of cells in the regions that were not treated by PAO demonstrated that (i)  $\sim 50\%$  of cells died in the wells that were surrounded by four PAO-containing wells. (ii) 10–30% of cells died in the wells that had 1–3 adjacent PAO-containing wells. From the dose–response curve (Figure 3), we estimated that the wells in which 50% of cells died contained  $\sim 0.4 \mu\text{M}$  PAO, a concentration that plausibly diffused from the four adjacent wells containing 250  $\mu\text{M}$  PAO. Taking into account the relative volumes of the wells, we concluded that  $<0.05\%$  of the PAO in the well diffused to a neighboring well over a 24-h period. Diffusion through PDMS-patterned paper or through siloxane-based gaskets was not unexpected because diffusion of small, hydrophobic organic molecules through PDMS is well-known.<sup>34</sup> This test revealed trace leakage that was not obvious under previous, less stringent conditions.

Experiments that use a 500-fold excess of cytotoxic compound (i.e., 500 times the minimum concentration required to induce cell death) that is present in four adjacent wells are unlikely in chemical screens. Since most high-throughput chemical screens are optimized to contain fewer than 10% hits per each plate, identifying a few wells that influence neighboring wells through between-well leakage should be relatively simple. The assays that involve small,

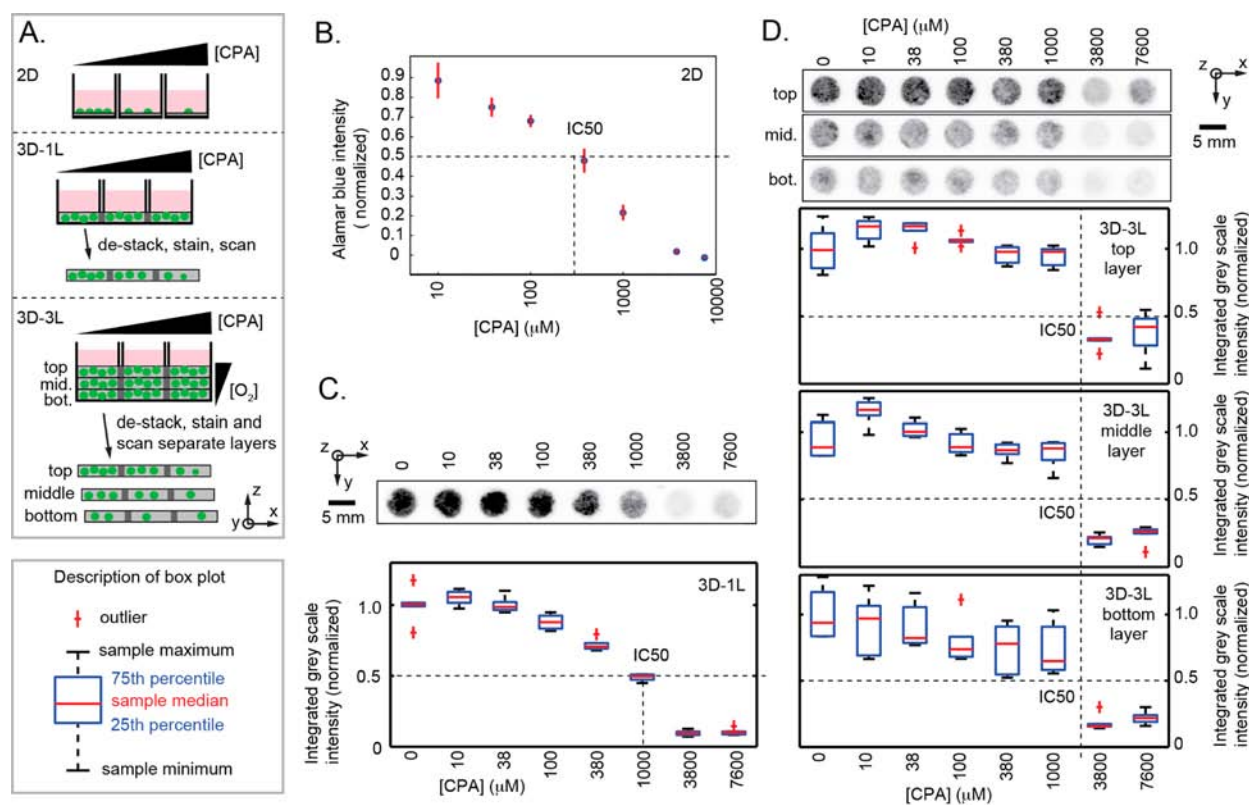


**Figure 5.** Long-term exposure of 3D cell cultures to cyclophosphamide (CPA). (A) Scheme describes 2D and 3D constructs made of single (1 L, 200 μm thick) and three layers (3 L, 3 × 200-μm thick). All constructs were exposed to CPA for 3 days. (B) In 2D culture, MDA-MB-231 cells were killed by CPA over the course of 3 days with an apparent IC<sub>50</sub> of 300 μM. We estimated the number of live cells using Alamar Blue; the intensities were normalized with respect to the wells containing no CPA. Blue circles represent an average of six experiments; red bars are 2 × (standard deviation). (C) Image of the cells in paper from 3D-1L constructs; black color is proportional to the fluorescent intensity of calcein staining. Each cell-containing zone was exposed to the indicated concentration of CPA. The box plot describes the normalized gray scale intensities of cell-containing zones from six replicates. IC<sub>50</sub> is 1000 μM. The legend (left) describes the statistical values represented by the box plot. (D) Representative images of the layers from 3D-3L constructs. The box plots describe normalized gray scale intensities of cell-containing zones in different layers. Estimated IC<sub>50</sub> is 3000 μM for all three layers.

nonpolar molecules could be rerun in two different configurations to account for trace leakage of highly potent molecules (i.e., those that are present at concentrations exceeding the EC<sub>50</sub> or IC<sub>50</sub> of these molecules by >100-fold). We predict that these assemblies will require no correction or retesting (at least to correct for lateral diffusion) for assays that utilize large polar biomolecules, such as proteins or siRNAs, which cannot diffuse through siloxanes, and plausible also through the hydrophobic pores in wax-printed regions. For other type of high-throughput screens, different materials can be used to obtain the most suitable 96-well holder, and we demonstrated that other gasket materials (with permeability lower than siloxanes), and other kind of patterned layers, could be used.

**Performance of the 96-Well Holder in Long-Term Culture Experiments.** To assess whether the platform can be used in long-term culture experiments, we performed a 3-days-long cytotoxicity titration in the presence of different concentrations of the anticancer drug cyclophosphamide (CPA). We compared the 2D culture with 3D constructs of 200- and 600-μm thickness. Figure 5 displays the results of the experiments in these three conditions (Figure 5A). In short, we observed that the IC<sub>50</sub> of CPA required to kill MDA-MB-231 cells in 3D cultures (Figure 5C,D) was a factor of 3–10 higher than the IC<sub>50</sub> for the same drug and the same cells in 2D culture (Figure 5B). Statistically significant different responses

from wells that contained lethal and sublethal doses of CPA confirmed that there is no significant leakage of CPA over the course of 3 days. A small amount of cross-well leakage might have occurred (<1% according to Figure 4), but it did not affect the experiment performed over multiple days. We also confirmed the results by confocal microscopy (Figure S4 in the Supporting Information). We observed the population of cells in 3D, 200-μm constructs for various concentrations around the IC<sub>50</sub> of CPA (e.g., 380 μM, 1000 μM, and 3800 μM). A similar comparison between 2D culture and 3D constructs was realized with long-term exposure to paclitaxel (Figure S5 in the Supporting Information).

## CONCLUSIONS

The system for parallel arrays of three-dimensional cell culture described here combines the advantages of CiGiP with the convenience of standard multiwell format. Unlike existing screening platforms that mimic 3D tissues, paper-based cultures can be easily separated into 200-μm-thick sections (slabs) for optical or fluorescent analysis. The 96-well holder with the footprint expected for a standard 96-well plate is compatible with commercial instruments used for high-throughput plating and analysis (e.g., multichannel dispensers, and plate readers).

The design of the holder has the potential to enable the manufacturing of the components at low-cost using standard technique (e.g., injection molding, printing). Both the single-

well dish and the 96-hole insert have simple shapes and will be easy to fabricate by injection molding. Tapping holes in the single-well dish is the only finishing step required after injection molding, and this process is easily automated. If molded from the appropriate material (PMMA), the 96-well holder can be sterilized in an autoclave. The parts, hence, can be reused if necessary.

We envision two immediate challenges in the development of this device for large-scale use: The first challenge, one involving materials science, is the identification of an elastomer and materials for patterning of paper that prevent diffusion of all types of molecules (including small hydrophobic molecules and gases, especially oxygen) between adjacent wells, either across the surface of sheets or laterally between wells. Although wax-patterned paper allows slow diffusion of oxygen<sup>29</sup> and small hydrophobic molecules between wells, the current 96-well holder, we believe, is suitable for many high-throughput screening assays that test the function of biomolecules and small organic molecules on cell function using assays that require several days of culture. Modification of the 96-well holder, by using other materials and with improved methods of fabrication, should completely eliminate leaking and allow long-term assays (e.g., multiple weeks) with large excesses of nonpolar molecules that readily diffuse through standard rubbers and elastomers. We believe that this challenge can be solved by using materials that are not permeable to organic molecules (for example, elastomers based on fluorocarbons).

The second challenge, one requiring a mechanical engineering solution, is the design of a reversible assembly–disassembly system that can replace the 15 bolts that we used to fasten the top and the bottom halves of the holder, with a simple compression closure and clamp. Although it takes ~30 s to fasten all bolts with an automated torque-sensitive screw driver, this step can be simplified if the top and bottom halves can be gripped by pins or ratchets or using other techniques for closure that do not require fastening of bolts.

The device presented in this article is the first functional prototype that allowed chemical screening in multilayer 3D cultures. Because it integrates seamlessly with the existing infrastructure for 96-well plates, we anticipate that it will find use in academic and industrial laboratories and facilitate the development of screening assays based on 3D tissue culture.

## ■ ASSOCIATED CONTENT

### ● Supporting Information

Additional information as noted in text. This material is available free of charge via the Internet at <http://pubs.acs.org>.

## ■ AUTHOR INFORMATION

### Corresponding Author

\*E-mail: [ratmir.derda@ualberta.ca](mailto:ratmir.derda@ualberta.ca) (R.D.); [gwhitesides@gmwhgroup.harvard.edu](mailto:gwhitesides@gmwhgroup.harvard.edu) (G.M.W.).

### Notes

The authors declare no competing financial interest.

## ■ ACKNOWLEDGMENTS

This work was supported by the Wyss Institute of Biologically Inspired Engineering, Vertex Inc., the Bill and Melinda Gates Foundation, the National Institutes of Health Grant ES 016665 (to G.M.W.), and the DOD Breast Cancer Innovator Award BC074986 (to D.E.I.). R.D. acknowledges University of Alberta Startup Funds and Canada Foundation for Innovation (CFI)

for infrastructure support, Alberta Glycomics Centre for salary support to F.D., and John Mackey (Alberta, Oncology) for samples of cyclophosphamide and paclitaxel.

## ■ REFERENCES

- (1) Pampaloni, F.; Reynaud, E. G.; Stelzer, E. H. K. *Nat. Rev. Mol. Cell Biol.* **2007**, *8*, 839–845.
- (2) Cukierman, E.; Pankov, R.; Yamada, K. M. *Curr. Opin. Cell Biol.* **2002**, *14*, 633–639.
- (3) Torisawa, Y.; Shiku, H.; Yasukawa, T.; Nishizawa, M.; Matsue, T. *Biomaterials* **2005**, *26*, 2165–2172.
- (4) Schmeichel, K. L.; Bissell, M. J. *J. Cell Sci.* **2003**, *116*, 2377–2388.
- (5) Sutherland, R. M. *Science* **1988**, *240*, 177–184.
- (6) Weaver, V. M.; Petersen, O. W.; Wang, F.; Larabell, C. A.; Briand, P.; Damsky, C.; Bissell, M. J. *J. Cell Biol.* **1997**, *137*, 231–245.
- (7) Gobaa, S.; Hoehnel, S.; Roccio, M.; Negro, A.; Kobel, S.; Lutolf, M. P. *Nat. Methods* **2011**, *8*, 949–955.
- (8) Wen, Y.; Zhang, X.; Yang, S.-T. *Biotechnol. Prog.* **2010**, *26*, 1135–1144.
- (9) Griffith, L. G.; Swartz, M. A. *Nat. Rev. Mol. Cell Biol.* **2006**, *7*, 211–224.
- (10) Flaim, C. J.; Teng, D.; Chien, S.; Bhatia, S. N. *Stem Cells Dev.* **2008**, *17*, 29–40.
- (11) Underhill, G. H.; Bhatia, S. N. *Curr. Opin. Chem. Biol.* **2007**, *11*, 357–366.
- (12) Fernandes, T. G.; Diogo, M. M.; Clark, D. S.; Dordick, J. S.; Cabral, J. M. S. *Trends Biotechnol.* **2009**, *27*, 342–349.
- (13) Tung, Y.-C.; Hsiao, A. Y.; Allen, S. G.; Torisawa, Y.-s.; Ho, M.; Takayama, S. *Analyst* **2010**, *136*, 473–478.
- (14) Montanez-Sauri, S. I.; Sung, K. E.; Puccinelli, J. P.; Pehlke, C.; Beebe, D. J. *J. Lab. Autom.* **2011**, *16*, 171–185.
- (15) Lee, M. Y.; Kumar, R. A.; Sukumaran, S. M.; Hogg, M. G.; Clark, D. S.; Dordick, J. S. *Proc. Natl. Acad. Sci. U.S.A.* **2008**, *105*, 59–63.
- (16) Fernandes, T. G.; Kwon, S. J.; Bale, S. S.; Lee, M.-Y.; Diogo, M. M.; Clark, D. S.; Cabral, J. M. S.; Dordick, J. S. *Biotechnol. Bioeng.* **2010**, *106*, 106–118.
- (17) Lii, J.; Hsu, W.-J.; Parsa, H.; Das, A.; Rouse, R.; Sia, S. K. *Anal. Chem.* **2008**, *80*, 3640–3647.
- (18) Berthier, E.; Surfus, J.; Verbsky, J.; Huttenlocher, A.; Beebe, D. *Integr. Biol.* **2010**, *2*, 630–638.
- (19) Young, E. W. K.; Beebe, D. J. *Chem. Soc. Rev.* **2010**, *39*, 1036–1048.
- (20) Meyvantsson, I.; Beebe, D. J. *Annu. Rev. Anal. Chem.* **2008**, *1*, 423–449.
- (21) Sung, K. E.; Yang, N.; Pehlke, C.; Keely, P. J.; Eliceiri, K. W.; Friedl, A.; Beebe, D. J. *Integr. Biol.* **2011**, *3*, 439–450.
- (22) Cukierman, E.; Pankov, R.; Stevens, D. R.; Yamada, K. M. *Science* **2001**, *294*, 1708–1712.
- (23) Yamada, K. M.; Cukierman, E. *Cell* **2007**, *130*, 601–610.
- (24) Horning, J. L.; Sahoo, S. K.; Vijayaraghavalu, S.; Dimitrijevic, S.; Vasir, J. K.; Jain, T. K.; Panda, A. K.; Labhasetwar, V. *Mol. Pharmaceutics* **2008**, *5*, 849–862.
- (25) Justice, B. A.; Badr, N. A.; Felder, R. A. *Drug Discovery Today* **2009**, *14*, 102–107.
- (26) Thurber, G. M.; Schmidt, M. M.; Wittrup, K. D. *Adv. Drug Delivery Rev.* **2008**, *60*, 1421–1434.
- (27) Minchinton, A. I.; Tannock, I. F. *Nat. Rev. Cancer* **2006**, *6*, 583–592.
- (28) Derda, R.; Laromaine, A.; Mammoto, A.; Tang, S. K. Y.; Mammoto, T.; Ingber, D. E.; Whitesides, G. M. *Proc. Natl. Acad. Sci. U.S.A.* **2009**, *106*, 18457–18462.
- (29) Derda, R.; Tang, S. K. Y.; Laromaine, A.; Mosadegh, B.; Hong, E.; Mwangi, M.; Mammoto, A.; Ingber, D. E.; Whitesides, G. M. *PLoS ONE* **2011**, *6* (5), e18940.
- (30) Carrilho, E.; Martinez, A. W.; Whitesides, G. M. *Anal. Chem.* **2009**, *81*, 7091–7095.

- (31) Bruzewicz, D. A.; Reches, M.; Whitesides, G. M. *Anal. Chem.* **2008**, *80*, 3387–3392.
- (32) Bailey, S. N.; Sabatini, D. M.; Stockwell, B. R. *Proc. Natl. Acad. Sci. U.S.A.* **2004**, *101*, 16144–16149.
- (33) Bogumil, R.; Namgaladze, D.; Schaarschmidt, D.; Schmachtel, T.; Hellstern, S.; Mutzel, R.; Ullrich, V. *Eur. J. Biochem.* **2000**, *267*, 1407–1415.
- (34) Lee, J. N.; Park, C.; Whitesides, G. M. *Anal. Chem.* **2003**, *75*, 6544–6554.